

SOME THEORETICAL APPLICATIONS TO ORGANIC CHEMISTRY

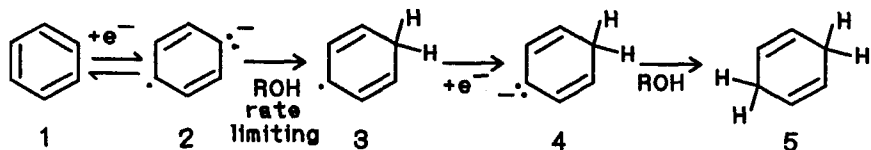
HOWARD E. ZIMMERMAN
*Chemistry Department, University of Wisconsin
 Madison, WI 53706*

The material in this chapter is a survey of some theoretical concepts, ideas and methods introduced in our research. Most of the theory has been in conjunction with experimental results. Thus, theory has proven especially useful in understanding ground state chemistry and much more essential in interpreting excited state behavior.

1 Ground State Examples

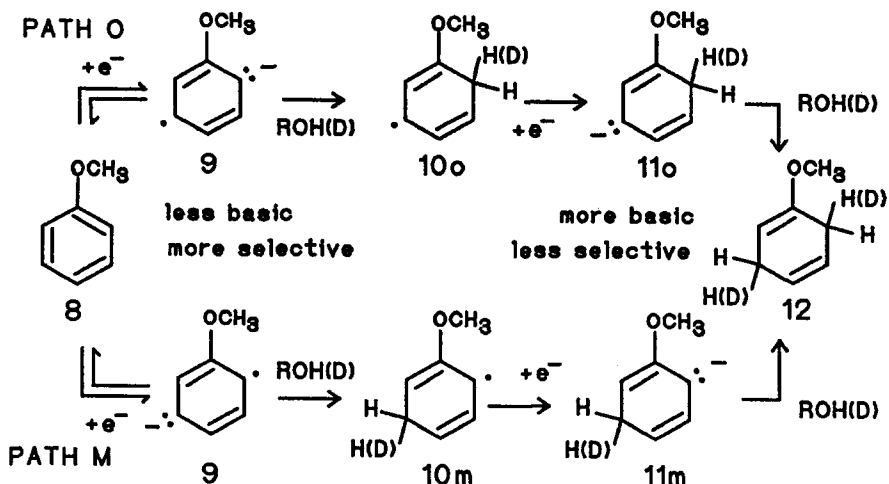
1.1 The Birch Reduction

The basic mechanism of the Birch Reduction,¹ as postulated by Birch, involved a one-electron reduction to give the radical-anion, followed by subsequent protonation of this species by an alcohol, introduction of a second electron, and finally a second protonation step. The kinetics reported by Krapcho and Bothner-by² established that the rate-limiting step is the protonation of the radical-anion **2**. However, what was controversial was the regioselectivity of that initial protonation step. The original Birch



mechanism suggested, on a qualitative basis, that the site of greatest negative charge and thus the initial protonation was at the meta position in alkoxyated and alkylated benzenes (e.g. anisole, compound **8** in Scheme I). However, in our very early studies,³ simple Hückel calculations were the best available and these were used to probe the electron densities for a variety of alkoxyated aromatics. It was found that it was invariably the ortho position which was the site of highest density in the radical-anion. This became a controversial topic, and the views on the two mechanisms shown in Scheme I oscillated over the years. Finally, in more recent research⁴ we obtained experimental evidence indicating that ortho protonation was preferred seven to one. Since more modern computational methodology was available, Gaussian90^{5a} and Gamess^{5b} (ROHF/3-21G) were used with the result that the electron density at the ortho position was found to be 1.302 versus 1.259 at the meta one. Interestingly, the frontier MO coefficients (i.e. the singly occupied antibonding MO) did not correlate with

experiment. Additionally, the energy of the ortho-protonated species proved to be lower than that of the meta-protonated counterpart. Similar results were obtained with alkyl substitution.



Scheme I: Possible mechanisms for the Birch reduction of anisole.

With regard to the second protonation step in the Birch reduction, wherein the central site of a cyclohexadienyl carbanion is protonated at the central carbon giving the unconjugated Birch product, we note that this is a general phenomenon. The highest electron density is obtained at the central carbon. This has precedent in the case of the dienolates obtained from enones⁶ where kinetic protonation of the dienolate affords the thermodynamically less stable β,γ -enone.

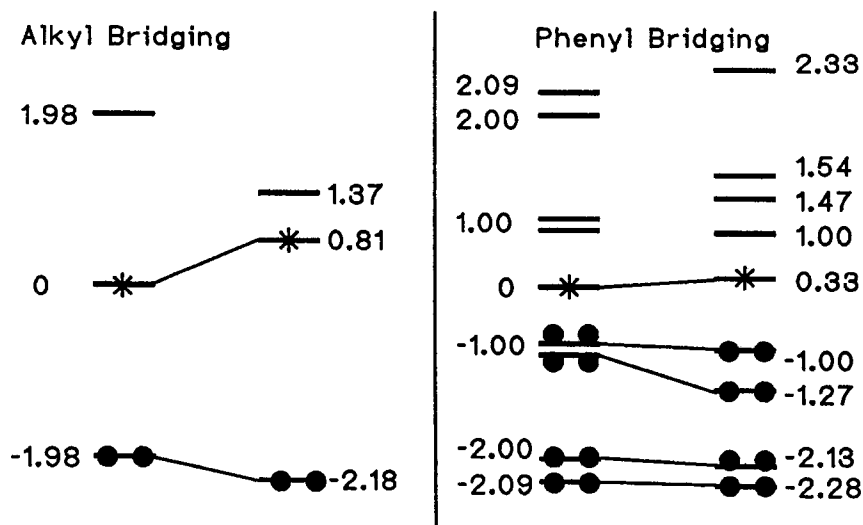
Several points should be noted. First, use of frontier MO reasoning runs a risk of giving incorrect predictions. Secondly, Hückel computations are generally of real value. Hückel theory is synonymous with graphic theory and reflects topology. While more sophisticated computations are needed, in many cases Hückel results give insight to the electronics of molecular systems.

1.2 1,2-Carbanion Rearrangements

While 1,2 carbon to carbon shifts of alkyl and aryl groups are common for carbocations, the corresponding odd-electron and carbanions case are more rare. The electronic

rationale for this behavior was noted by the present author in 1961.⁷ Interestingly, this paper presented the first correlation diagram for an organic reaction; note Scheme II. A group was considered to migrate from carbon-1 to carbon-2, and the computations used a truncated basis set. This set was comprised of two p-orbitals and an sp^2 hybrid for the alkyl migration and a total of nine localized basis orbitals for the phenyl migration where there were six p-orbitals in the aromatic ring. One in-plane sp^2 -hybrid at the ring carbon originally bonded to carbon-1 and one localized orbital was taken at each of C-1 and C-2 as shown in Figure 1. The correlation diagram considered the starting MO's and those of the half-migrated species, either with an alkyl group (e.g. methyl) half-migrated from C-1 to C-2 or with the phenonium intermediate being formed. The solid dots indicate electron occupation in the MO's and the asterisk represents zero electrons for the carbocation case, one electron for the free radical situation, or two electrons for a carbanion rearrangement.

It is seen that for a carbanion, the two non-bonding electrons taken as at an energy defined as zero, become badly anti-bonding where an alkyl group as methyl is migrating. However, for the phenyl migration, the rise in energy is much smaller. This was shown to be a general situation with further variation in substitution [also see Ref 8 for more details].



Scheme II: Correlation diagrams for alkyl and phenyl migration; reactant and half-migrated species given.

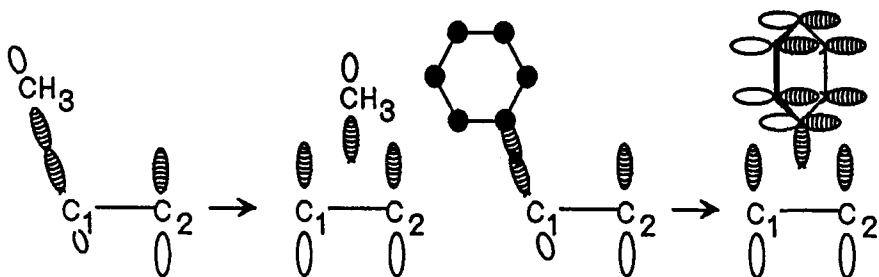


Figure 1: Basis Set Orbitals for Methyl and Phenyl 1,2-Migrations.

1.3 The Möbius-Hückel Concept

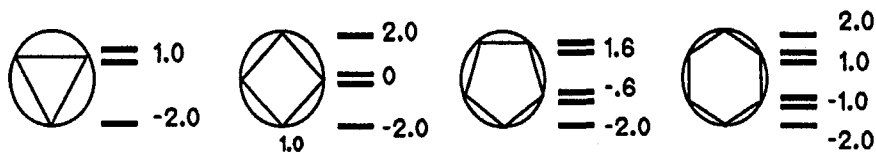
The idea of allowedness vs. forbiddenness, or aromaticity vs anti-aromaticity, of pericyclic reactions was advanced by Woodward and Hoffmann⁹ and Longuet-Higgins and Abrahamson.¹⁰ Edgar Heilbronner¹¹ had published a paper noting that a twisted, Möbius cyclic annulene would have a set of MO's which differed from that cyclic Hückel systems; and a counterpart algebraic formula for these twisted annulenes was given. Unlike the Hückel systems, the twisted annulenes preferred having $4N$ electrons for a closed shell. However, as a consequence of the twisting, the energies were never lower than that of the corresponding Hückel counterpart.

With this as background, the present author¹² suggested that for reaction transition states where alternative geometries, Hückel and Möbius, had equal twisting and equal diminution of overlap between adjacent basis set orbitals, one would find Möbius systems to be preferred as transition states when $4N$ electrons were delocalized while Hückel systems would be preferred, as expected, when there were $6N$ electrons.

For Möbius a circle mnemonic was presented¹² which was the counterpart of the well-known Frost-Musulin¹³ device for Hückel systems. These mnemonics are shown in Figure 2 for the case of a four orbital system. The Möbius mnemonic differs from the Frost-Musulin one in requiring a polygon 'side' down rather than a vertex at the bottom of the circle as for Hückel systems. Note Figure 2.

To identify Möbius and Hückel systems, given a cyclic array of basis set orbitals, in an actual molecule or in a transition state, one needs to count the number of sign inversions between pairs of basis set orbitals. With zero or an even number of such inversions, the system is of the Hückel variety. With an odd number (e.g. 1), the system is a Möbius one.

HÜCKEL SYSTEMS:



MÖBIUS SYSTEMS:

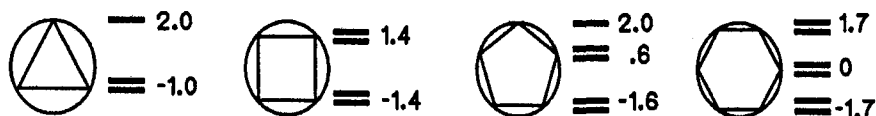


Figure 2: The Möbius - Hückel circle mnemonics.

For consideration of allowedness versus forbiddenness, one can write the cyclic array for a given pair of pericyclic reaction transition states, populate the MO's, and then compare energies of the Hückel and the Möbius counterparts. The lower energy one is the allowed reaction pathway. More interestingly, one can develop the correlation diagram for the reactions without the use of symmetry. This is done by recognizing that for each degenerate pair in the transition state, there is a crossing of a set of MO's as one proceeds from reactant to product.

Figures 3 and 4 give one example. This shows that the opening of cyclobutene to give butadiene in the ground state will prefer a conrotatory pathway as opposed to a disrotatory one (Note Figure 4), in which a Möbius transition state is employed. The correlation diagram for both conrotatory and disrotatory reactions is readily drawn by obtaining the transition state degeneracies from the circle mnemonics and recognition that each degeneracy gives rise to crossing of two MO's. The conrotatory mechanism leaves all of the bonding MO's as bonding while the disrotatory mechanism converts a bonding MO to an antibonding one. Thus if one were to picture the first-order situation of an adiabatic reaction (i.e. before any configuration interaction), a ground state reactant proceeding in a disrotatory fashion would afford a very high energy doubly excited state of product.

The Möbius-Hückel concept applies to more than the transition states discussed above. There are many Möbius molecules already known. One is barrelene. This molecule has three ethylene bridges. One may start with the bonding MO's of ethylene

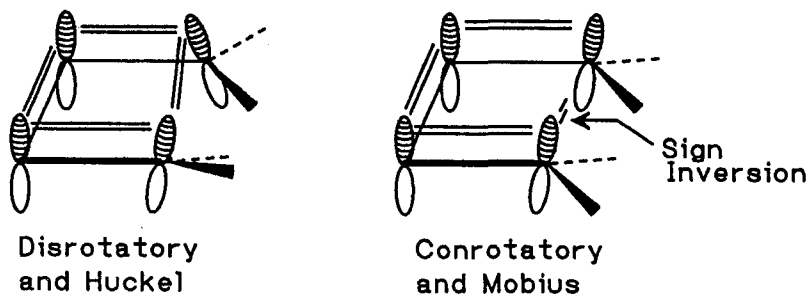


Figure 3: Basis set orbitals and twisting of Möbius and Hückel transition states for cyclobutene opening.

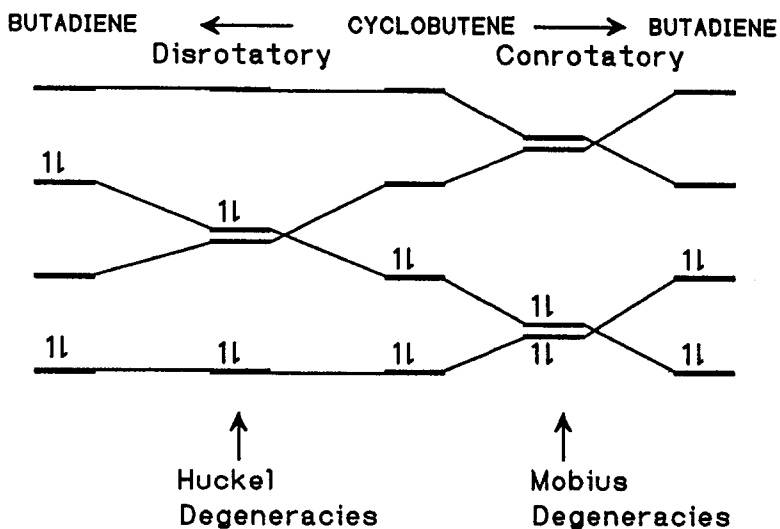


Figure 4: Correlation diagram interconverting cyclobutene and butadiene by conrotatory and disrotatory twisting.

on each bridge and note that these interact in a Möbius fashion. At a simple Hückel level, the bonding MO of ethylene is at -1 , the energy scale using units of the absolute value of β . The transannular overlap is less by a factor (ϵ) than that for two adjacent p-orbitals. The Möbius splitting of the three bonding MO's thus results in a degenerate pair of MO's at $-1 - \epsilon$ and a single MO at $-1 + 2\epsilon$. This is illustrated in Figure 5. Similar consideration of the antibonding ethylenic orbitals as a basis set, leads to a similar splitting about the antibonding ethylenic MO at $+1$. Note Figure 5.

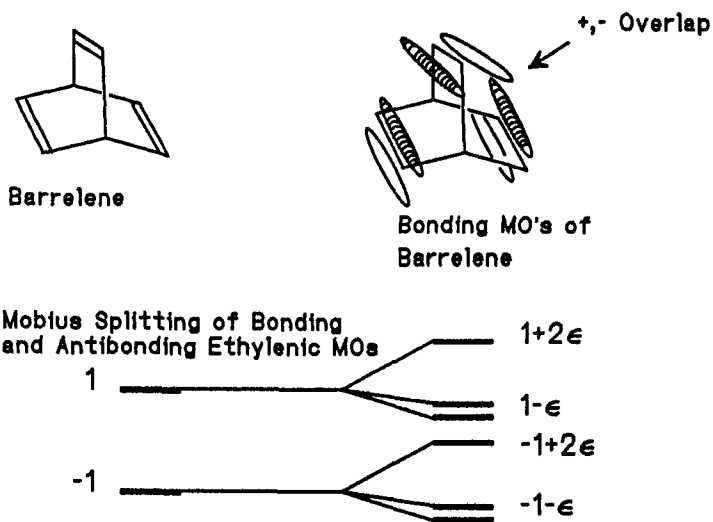


Figure 5: Admixture of three ethylene bridges of barrelene.

1.4 Prediction of Organic Reactions Using Group-Group Polarizability

In Hückel theory bond-bond, atom-bond, bond-atom, and atom-atom polarizabilities give the change in one part of the molecule as another is modified. For example, in bond-bond polarizability, one obtains the change in a bond order (e.g. r-s) as the resonance integral β is changed for another pair of atoms (e.g. t-u). In the case of atom-atom polarizability, one obtains the change in charge at one center as the Coulomb integral at another atom is modified. The atom-bond and bond-atom parameters are defined similarly.

While these polarizabilities¹⁴ are of intellectual interest, they have had severe limitations. (a) They have been limited to use with π -systems (e.g. aromatics), (b) the neglect of overlap approximation has assumed different p-orbitals do not overlap, (c) and the approximate nature of Hückel wavefunctions is generally a problem.

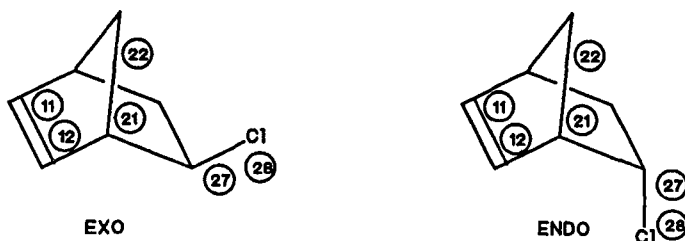
It was recognized by the author¹⁵ that the mutual-polarizability concept could be applied to organic molecules in general, including those having both sigma and pi bonds. Further, the most modern self-consistent field methods could be employed, not only the more approximate semi-empirical wavefunctions, but also *ab initio* ones. This was made possible by the realization that Weinhold "natural hybrid orbitals" (i.e. NHO's)¹⁶ comprise an orthogonal basis unlike a Hückel set. Additionally, the NHO basis orbitals are readily available from both semi-empirical computations (e.g. AM1)

and ab initio ones (e.g. 3-21G, 6-31G*, etc.). A minor addition is required wherein the ϵ_{rs} and ϵ_{tu} elements included are +1 or -1 depending on the basis set overlap and were obtained from the Fock matrix signs for off-diagonal elements. Thus the bond-bond polarizabilities are given in Equation 1.

$$P(r,s,t,u) = \epsilon_{rs} \epsilon_{tu} \sum_k^{occ} \sum_l^{vir} \frac{(C_{rk} C_{sl} + C_{rl} C_{sk}) (C_{ik} C_{ul} + C_{il} C_{uk})}{(E_l - E_k)} \quad (1)$$

However, the application to chemical reactivity relies on recognizing in the molecule some group which is weakening or strengthening and hence initiating a reaction. Then group-group polarizability indicates the response of all other bonds and atoms in molecule. The result is a parallel to ordinary electron pushing; however, the method provides a quantitative prediction of molecular changes. For example, if there is a potentially departing tosylate moiety held by bond r-s, one can determine which other bonds will respond to tosylate loss by weakening and which bonding will be enhanced. Similarly, one can see what molecular sites become more electron deficient in such a case.

While a number of examples were given, one representative example is the solvolysis of exo- and endo-norbornyl chloride.¹⁷ It is well known that the exo stereoisomer solvolyses in polar media much more rapidly than the endo isomer. Also, there is evidence for participation of the π -bond.



Scheme III: The exo and endo norbornenyl systems with labeled orbitals.

We see interaction between the π -bond 11-12 and the C-Cl sigma bond with a positive polarizability (0.00575) in the case of the exo stereoisomer compared with essentially zero for the endo isomer. The positive value for the exo isomer indicates withdrawal of electron density and weakening of C=C π -bond 11-12 as the C-Cl sigma bond (27-28) is broken. The difference between the exo and endo isomers, again, correlates with the experimental behavior of the two compounds on solvolysis. One

Table 1: Exo and endo dehydronorbornyl bond-bond polarizabilities.

Exo Norbornenyl Polarizabilities

r	s	t	u	Orb r	Orb s	Orb t	Orb u	Polarizability
27	28	11	12	C 5(Cl 8)	Cl 8(C 5)	C 2(C 3)	C 3(C 2)	0.005753
27	28	21	22	C 5(Cl 8)	Cl 8(C 5)	C 4(C 7)	C 7(C 4)	0.000723
28	28	11	12	Cl 8(C 5)	Cl 8(C 5)	C 2(C 3)	C 3(C 2)	-0.000429
28	28	22	22	Cl 8(C 5)	Cl 8(C 5)	C 4(C 7)	C 7(C 4)	-0.000547

Endo Norbornenyl Polarizabilities

r	s	t	u	Orb r	Orb s	Orb t	Orb u	Polarizability
27	28	11	12	C 5(Cl 8)	Cl 8(C 5)	C 2(C 3)	C 3(C 2)	-0.000092
27	28	21	22	C 5(Cl 8)	Cl 8(C 5)	C 4(C 7)	C 7(C 4)	0.011229
28	28	11	12	Cl 8(C 5)	Cl 8(C 5)	C 2(C 3)	C 3(C 2)	0.000158
28	28	22	22	Cl 8(C 5)	Cl 8(C 5)	C 4(C 7)	C 7(C 4)	-0.008572

interesting facet is the heavy electron withdrawal from the sigma bond 21-22 in the endo stereoisomer (i.e. the chlorine is endo, note 27-28:21-22). Additionally, the sigma bond anti-coplanar with the C-Cl bond of the exo-stereoisomer exhibits an appreciably large interaction with that bond.

While it is true that the polarizabilities computed are related to an "overlap path" of conjugating basis orbitals between interacting groups, the role of electron affinity and availability at the various centers plays a large role as well. But then these are the factors which control reactivity.

Further, polarizabilities represent a precise counterpart to electron pushing and something which has not been considered in predicting reactivity of sigma systems. Beyond this, polarizabilities represent just one case where one can extend the Hückel treatment to sigma systems as a consequence of the orthogonality of the basis orbitals (i.e. NHO's) used.

1.5 Electron Density and Central Protonation of Mesomeric Anions

In the Birch Reduction discussed above, the final step was protonation of a mesomeric carbanion. Since we know that conjugated dienes are lower in energy than the unconjugated ones, formation of the unconjugated reaction product cannot be controlled by relative thermodynamic stability of the product. While in some reactions, the final product energy is seen sufficiently in the transition state, that the more stable product is the one formed. Not so here. It is observed as a general phenomenon that kinetic protonation of anions of the type $C=C-C=C-\underline{C}^- \leftrightarrow C=C-\underline{C}^-C=C \leftrightarrow \underline{C}^-C=C-C=C$ occurs at the central carbon. The same is true of dienolates such as $C=C-C=C-O^-$.

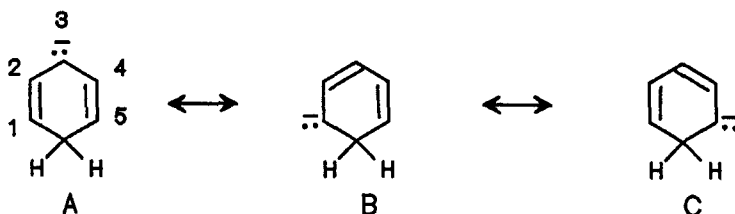


Figure 6: Three resonance structures for the cyclohexadienyl carbanion.

Simple Hückel calculations on the pentadienyl type anions predict an equal distribution of negative charge at atoms 1,3 and 5 (i.e. 0.333 e at each of the three centers) in agreement with the appearance of three resonance structures shown in Figure 6 for the example of the cyclohexadienyl carbanion. But in looking at the three resonance structures we note that two of the three structures have double bonds at C1-C2 and C4-C5 but single bonds at C2-C3 and C3-C4. Thus this qualitative resonance reasoning suggests that bond 1-2 and 4-5 should be shorter. In fact, if one adjusts the resonance integrals to reflect this, with the absolute value of the C1-C2 and C4-C5 values being larger, the electron density shifts towards C3. This is precisely what was done using the Mulliken-Wheland-Mann modification¹⁸ of Hückel theory in which the resonance integral β for bond r-s is given by Equation 2.

$$\beta_{rs} = \beta_0 [.08(P_{rs}(pi) + P_{rs}(sigma)) + 0.115] / 0.276 \quad (2)$$

$P_{rs}(sigma)$ was taken as unity while $P_{rs}(pi)$ is obtained from one iteration and then used in Equation 2 for the next iteration. The constants were selected so that with a π -bond order of unity, β_{rs} becomes equal to the standard β_0 . Although not here, in other applications, the Coulomb integral was also varied. Interestingly, Equation 2 is

philosophically related to the equations of SCF theory which is also iterative and where each successive iteration relies on the LCAO MO coefficients of the previous iteration.

More modern inspection of the mesomeric anions using the semiempirical AM1 and the ab initio Gaussian92 (and Gaussian94), is thus of real interest. Two alternative approaches have been considered.¹⁹ One is computation of the isolated mesomeric carbanions and the other is completion with the sodium cation included to give an ion-pair. Interestingly, both AM1²⁰ and Gaussian⁵ predict the highest electron density at the central atom for the ion pair in accord with experiment as well as for the simple carbanion. For the ion pair, one starts with the sodium cation positioned above either the central or the terminal carbon of the pentadienyl moiety. Geometry optimization moves the sodium cation until it is directly over the central carbon. These results are given in the first four columns of Table II.

Table II: Charge distribution in cyclohexadienyl anions (with and without the sodium cation present) and the cyclohexadienolate anion.

	Cyclohexadienyl		Na_cyclohexadienyl		Dienolate
	AM1	3-21G	AM1	3-21G	3-21G
1	-0.3669	-0.42178	-0.1723	-0.35756	-0.768332 (O)
2	-0.0487	-0.16345	-0.1192	-0.21866	0.520120
3	-0.3891	-0.57926	-0.0978	-0.70493	-0.460252
4	-0.0487	-0.16346	-0.1550	-0.21934	-0.169823
5	-0.3671	-0.42185	-0.1188	-0.35600	-0.330626

Also included are computations for the dienolate system. Experimentally, it is observed as a general phenomenon⁶ that protonation and alkylation bond to the carbon α to the carbonyl group ultimately engendered. While in this case the computations reveal the dienolate oxygen to be most electron rich, protonation at oxygen to afford the dienol is reversible and we need only consider the competition between (e.g.) protonation α to the incipient carbonyl group (i.e. numbered as C-3 below) versus γ to the carbonyl (i.e. at C-5); but C-3 is most electron rich, thus accounting for preferential protonation and alkylation at this site.

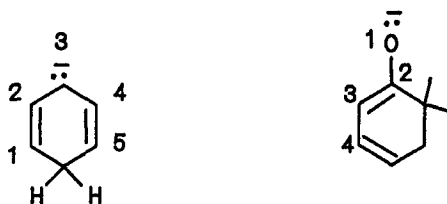


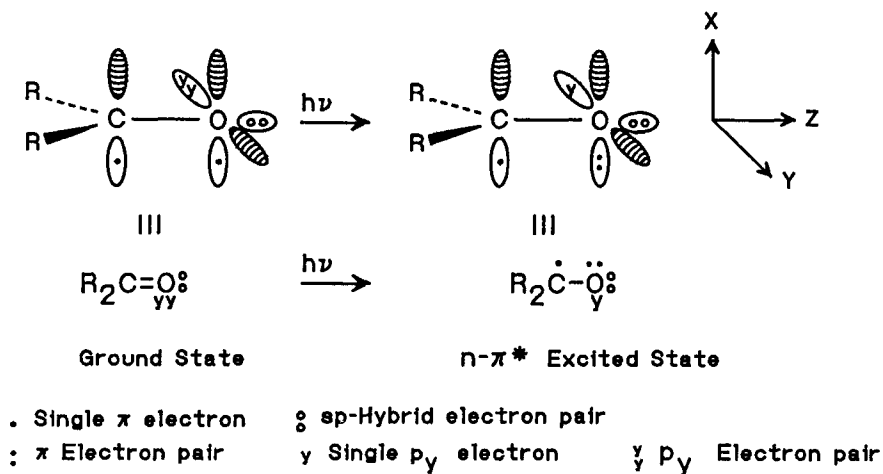
Figure 7: Cyclohexadienyl and dienolate anions.

2 Excited State and Open Shell Examples

2.1 $n-\pi^*$ Reactivity

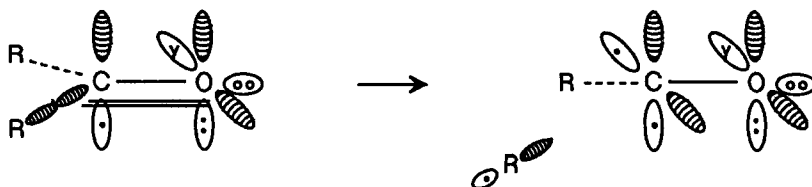
It was in 1961 that the present author suggested²¹ that $n-\pi^*$ singlets and triplets exhibit two types of photochemical reactivity and presented a general theory of excited state reactivity of organic species. This provided a basis for relating the three-dimensional electronic structure of a given excited state to possible photochemical transformations.

Of the two types of excited state reactions of $n-\pi^*$ states, one arises from the singly occupied p_y (or "n") orbital and the other from the π -system which has one extra, antibonding electron. The excitation process is shown in Scheme IV for a simple, unconjugated ketone. Since the p_y orbital is only singly occupied, it is highly electrophilic and quite willing to attack π -bonds and to abstract hydrogen atoms and

Scheme IV: $n-\pi^*$ excitation. Three-dimensional version above and Lewis structure equivalent below.

attack π -bonds. The hydrogen abstraction capability was independently reported by Kasha.²²

The p_y orbital of the $n-\pi^*$ excited state also has an "electron hole" which can be distributed in any coplanar σ -system. Thus, in the $n-\pi^*$ excited state this p-orbital is close to coplanar with the σ -bonds bonding alkyl groups to the carbonyl carbon. It was noted in our early work²¹ that delocalization of the "electron hole" leads to weakening of the sigma bond and thus accounts for the Norrish Type I cleavage which leads to an acyl and alkyl radical pair.

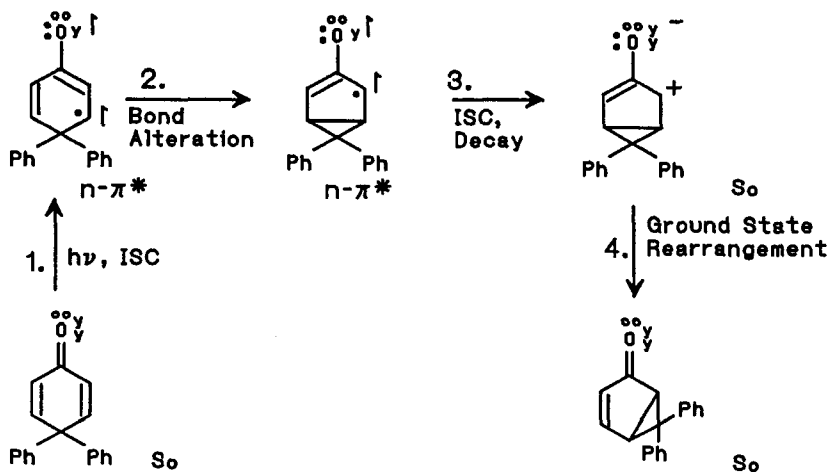


Scheme V: A basis orbital picture of the Norrish Type I cleavage reaction.

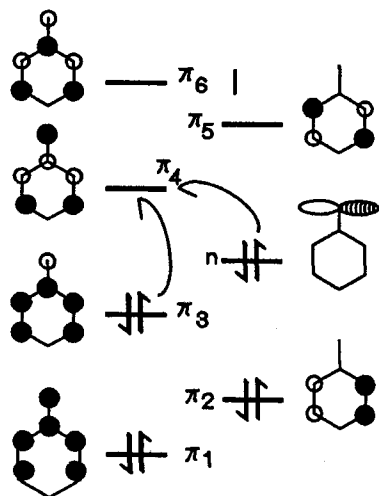
The second type of reactivity exhibited by $n-\pi^*$ excited states arises from the electron rich π -system which is isoconjugate with a radical anion. One example of a reaction of this class which was presented in that early study is the "Type A" Cyclohexadienone Rearrangement.²¹ The mechanism is outlined in Scheme VI. In this case, and in many others, there are four basic steps involved in the photochemistry. The first step is excitation and intersystem crossing (in this triplet example); intersystem crossing of ketones is a very rapid process. Step 2 is some molecular bond alteration; in the case of the Type A Cyclohexadienone Rearrangement, the molecular change involves $\pi-\pi$ bonding between the carbons β to the carbonyl group. Step 3 is radiationless decay, here by intersystem crossing to ground state; this step leads to a zwitterion. The last step 4 is a ground state process characteristic of the S_0 species engendered by Step 3. Here it is a rearrangement known²³ to occur from such zwitterion species.

While this is just one case of π -system reactivity of an $n-\pi^*$ excited state, we might stop and inspect some of the facets encountered. The first question is why the triplet excited state undergoes $\beta-\beta$ bonding. Scheme VII gives one view.²⁴ We see that in promotion of one electron from the p_y (or "n") orbital to MO 4, one has an excitation from an MO with a zero $\beta-\beta$ bond order to MO 4 which has an appreciable $\beta-\beta$ bond order. Thus $n-\pi^*$ excitation enhances the $\beta-\beta$ bond order. This is not true of promotion from MO 3 to MO 4 (i.e. a $\pi-\pi^*$ excitation) where both MOs are weighted positively at the β carbons and thus have positive bond orders. Our early computations used an

SCF-CI approach with a limited basis set comprised of the p_y and the π -system orbitals. These revealed that, of the triplet configurations, only the $n-\pi^*$ one is $\beta-\beta$ bonding. Interestingly S_0 is also bonding.



Scheme VI: Type A rearrangement mechanism.



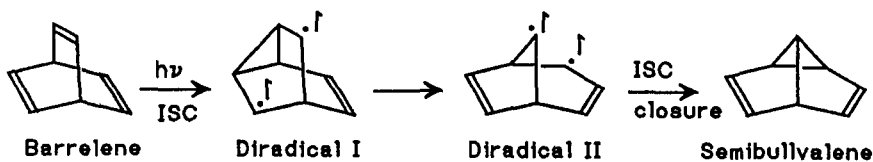
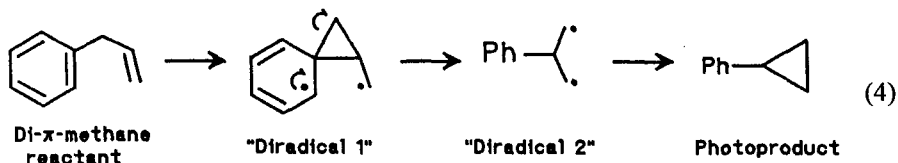
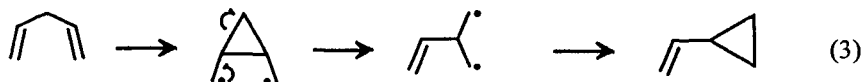
Scheme VII: $n-\pi^*$ and $\pi-\pi^*$ excitation processes. Solid orbitals are positive above the paper plane and white ones are negative above this plane.

2.2 π - π^* Reactivity

Of π - π^* excited state reactivity, the Di- π -Methane Rearrangement²⁵ provides one of the most common and most illustrative examples. The rearrangement was encountered in the rearrangement of barrelene to semibullvalene in 1965²⁵ but the correct mechanism and the generality of the reaction was realized only the next year.²⁶

The basic mechanism is depicted in Equations 3 and 4. The only requirement for the reaction is having two π groups bonded to a central sp^3 hybridized carbon. In Equation 3, both groups are taken as alkenyl and in Equation 4 one is pictured as an aryl group. Some examples of the Di- π -Methane Rearrangement proceed via a singlet excited state and some make use of the triplet.

An interesting case is the photochemical conversion of barrelene to semibullvalene as pictured mechanistically in Scheme VIII. It is seen that there are two bridgehead sp^3 hybridized carbons, each of which satisfies the requirement for two



Scheme VIII: The mechanism of the barrelene to semibullvalene conversion.

attached π -groups, here vinyls. In this case the experimental evidence is that the reaction proceeds via a triplet excited state. Also, at the outset there was evidence that "Diradical II" is an intermediate with a lifetime sufficient for conformational equilibration. Further, in this early work,^{26a,b} a reaction profile was obtained quantum mechanically by use of Extended Hückel computations.²⁷ Cartesian coordinates were

obtained for the reactant, product and diradical species from Dreiding molecular models taped to a piece of graph paper. The computations revealed both Diradical I and Diradical II to be energy minima and provided a limited hypersurface. A comparable computation for the originally assumed mechanism led to a vertical excited state in a deep minimum and faced with a large energy barrier.

However, much more recently with the availability of Gaussian90, G92 and G94, a more reliable computation was possible. This was done at the ROHF/6-31G* level for the triplet, RHF/6-31G* and then at the CASSCF(6,6)/6-31G* level in order to inspect more closely the effect of configuration interaction; this was done for both singlets and triplets.^{26c} Note Figures 8 and 9.

Several points are noteworthy. One is that despite the qualitative nature of the very early results, the vastly improved computations still confirmed the presence of two triplet energy minima with the structures of Diradicals I and II. The second point of interest is the near degeneracy of the triplet states (i.e. note the CASSCF results) of the

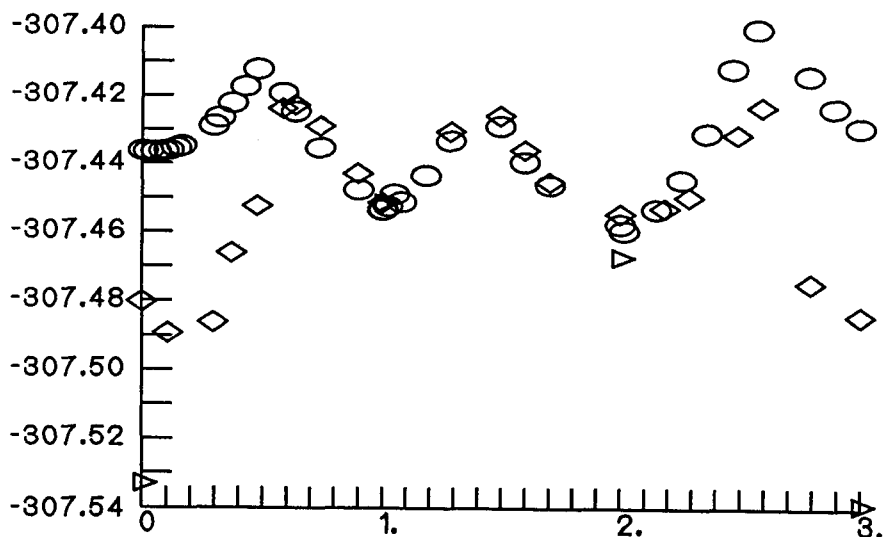


Figure 8: Triplet hypersurface for conversion of barrelene to semibullvalene including selected singlet points. The ordinate is in Hartrees. The abscissa is 0 for barrelene, 1 for diradical I, 2 for diradical II, and 3 for semibullvalene. The ellipsoids are for the triplet, the diamonds for the singlet with triplet geometry, the triangles for S0.

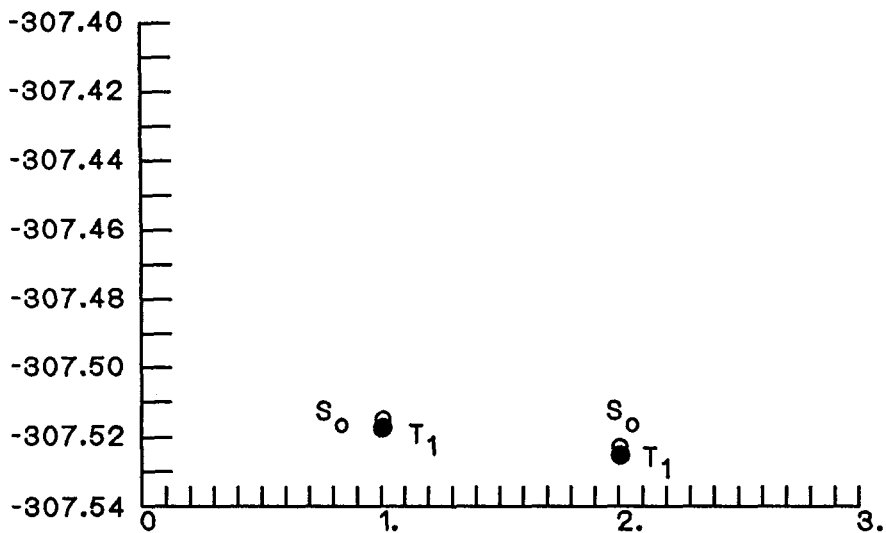
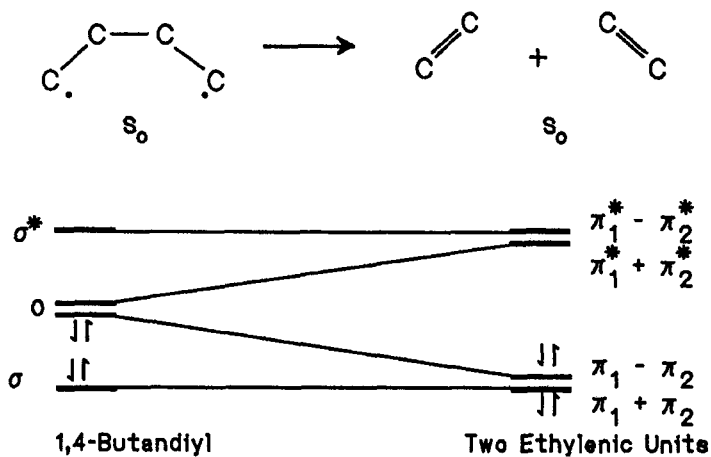


Figure 9: S_0 - T_1 near degeneracies for diradicals I and II.



Scheme IX: Facile allowed fragmentation of S_0 1,4-Diyls. In this scheme, the MO counterpart correlation diagram is depicted with an S_0 configuration.

diradicals with the ground state counterparts with the triplets being slightly lower in energy.

Another fascinating result was the finding that on attempting computation of the S_0 state of Diradical I with geometry optimization, the convergence was on the S_0 state of barrelene. That is, the computer had "run a reaction" leading the Diradical I structure back to that of barrelene; this corresponds to a well-known²⁸ reaction of S_0 1,4-diradicals in which bond 2-3 cleaves in an "allowed" process.

2.3 Conical Intersections, Funnels, Internal Conversion

For photochemical reactions proceeding via a singlet excited state, it was suggested by the present author²⁹ that the greatest probability of the reacting molecule to cross from the singlet hypersurface to ground state S_0 was where there are MO degeneracies between singly occupied antibonding MO's and singly occupied bonding MO's. Subsequently, this idea was treated in greater detail³⁰ and it was noted that the crossing of the two MO's is a conical intersection as described by Herzberg^{31a,c} and Longuet-Higgins.^{31b} This is depicted in Figure 10.

Such funnels have been found to be important in a variety of different transformations. Such funnels providing routes to ground state have been noted by Michl as well.³²

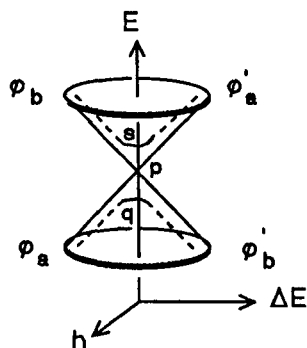
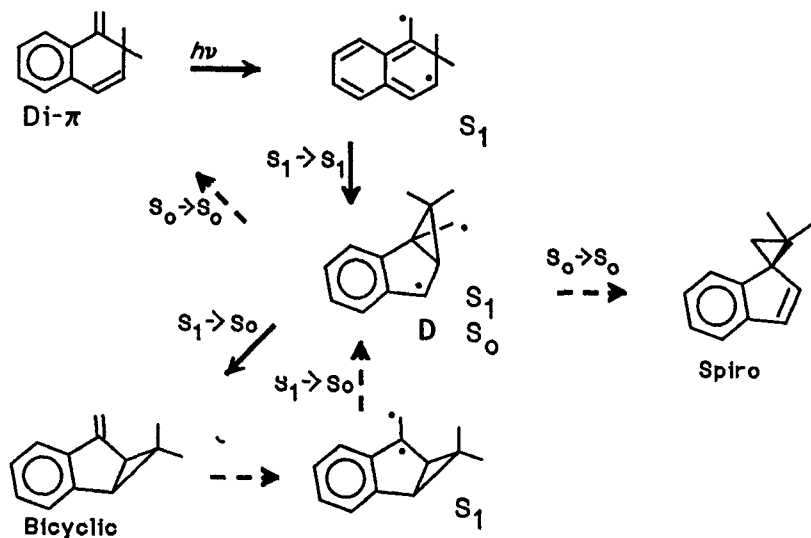


Figure 10. MO's becoming degenerate as a function of a reaction coordinate and energy splitting due to molecular deformation. 'k' represents the energy difference and thus a reaction coordinate, 'h' is a matrix interaction element resulting from molecular deformation. 'p' is the point of MO crossing. 's' and 'q' show the consequences of molecular deformation. The molecular deformation is likely as a consequence of a Jahn-Teller distortion.

In our own research, the role of these funnels in controlling the course of photochemical reactions has been noted in a variety of examples. One fascinating case is given in Scheme X.³³ This involves the photochemical singlet interconversion of three compounds. This provides an example of our Bicycle Rearrangement in which a carbon, part of a three-membered ring, moves stereospecifically along the π -surface of a molecule. The intriguing aspect of the case is presented in Scheme X. Here there are three compounds of interest, termed "Di- π ", "Bicyclic" and "Spiro" in Scheme X. "Spiro" is photochemically unreactive. However, "Di- π " and "Bicyclic" react by processes whose gross mechanisms are quite clear from the structural standpoint. The reactions beginning with "Di- π " are depicted with bold arrows while those which begin with "Bicyclic" are shown with dashed arrows. The paradox arises when we see that both the "Di- π " and the "Bicyclic" reactions need to proceed via diradical "D"; yet the reaction product depends on which reactant is employed. How can one intermediate (i.e. diradical "D") give rise to different behavior depending on its source?

While there are chemical momentum and trajectory considerations which, a priori might be involved, in this case there is another factor. Here two different states of diradical "D" proved to be involved. Those reactions beginning with reactant "Di- π " are indicated with solid arrows while those pathways initiated from reactant "Bicyclic" are shown with a dashed arrow.



Scheme X: Interconversion of three compounds, "Di- π ", "Bicyclic", and "Spiro".

The corresponding correlation diagram is given in Figure 11 which makes use of a triptych. Inspection of the correlation diagram reveals that the "Di- π " approach to Diradical "D" (i.e. using triptych branch A) involves no opportunity for loss of excitation, and this diradical is reached with an S_1 configuration. Conversely, the approach to Diradical "D" from "Bicyclic" reactant (i.e. using triptych branch B) affords a HOMO-LUMO crossing and thus an opportunity for radiationless decay to S_0 . The S_0 diradical "D" has allowed pathways leading to photoproducts "Di- π " and "Spiro". Finally, the excited state of "Spiro" can be seen to lead (adiabatically) to a doubly excited "D". Configuration Interaction leads us to a description in terms of states rather than MO's and this, too, has been carried out.³³ Where there are MO crossings, avoided crossings were obtained. Each such funnel affords an opportunity for radiationless decay to ground state. Thus whether one considers the problem in terms of MO's or states, the conclusion is the same. This treatment of the role of radiationless decay has been applied in a number of examples.³⁴ Additionally, related is the suggestion that a funnel may be canted and thus lead to a preference in the direction of motion on the ground state surface.^{33,34}

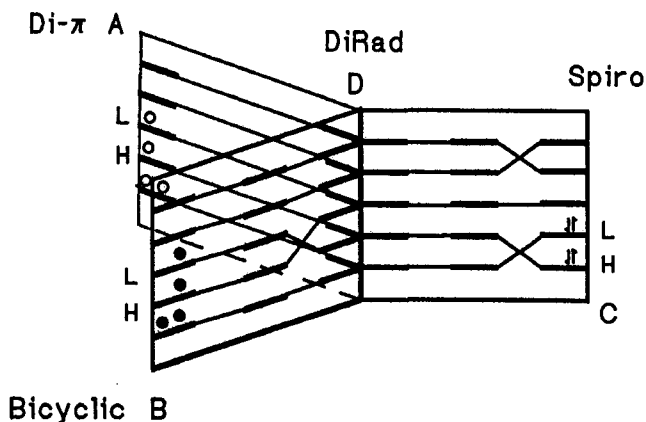
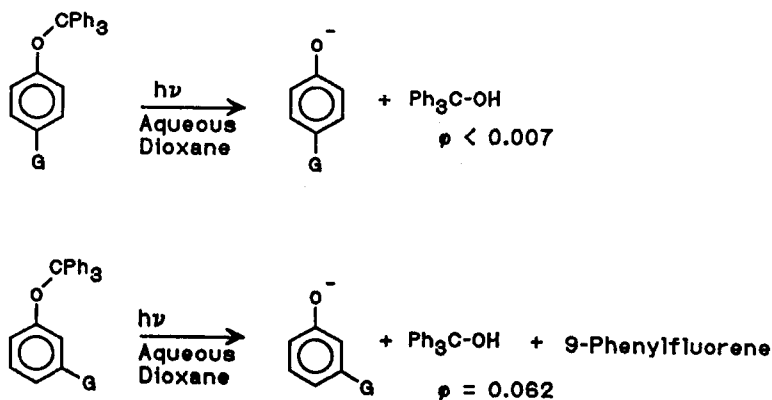


Figure 11: Molecular orbital correlation triptych.

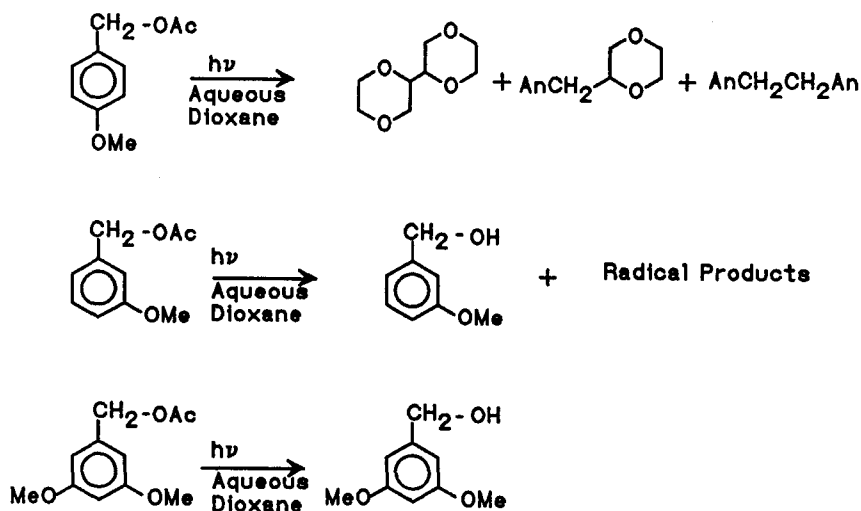
There are further aspects of conical intersections. The latest version of Gaussian94 contains very pretty programming by Robb to locate conical intersections and avoided crossings;³⁵ and examples where this has been successful have been presented by Bernardi, Robb and Coworkers.³⁶ This programming has permitted the study of the nature of the cations and radicals of the meta and para benzylic system discussed below in context of the "meta" effect.

2.4 The Meta Effect

It was observed originally by Havinga³⁷ that in the dark, meta-nitrophenyl phosphate hydrolyzed in water exceptionally slowly while the para isomer was quite reactive in giving rise to p-nitrophenol and phosphate; this is totally expected behavior as the p-nitrophenolate anion is much more delocalized and of lower energy than the meta counterpart. However, in light, the meta isomer hydrolyzed while the para counterpart was no more reactive than in the dark. This was said to be inexplicable in terms of ordinary resonance reasoning. This prompted the present author to make use of the then available Hückel computations and to determine the generality of the phenomenon. First note Scheme XI which depicts the facile expulsion of the trityl cation in the photolysis of m-nitrophenyl trityl ether but the much lower efficiency when the nitro group is para. In this solvolysis reaction, the trityl cation picks up either water or methanol depending on the reaction solvent.³⁸ For the electron donor counterpart, an example studied both experimentally and theoretically³⁹ was the solvolysis of meta-methoxy-phenyl acetate, para-methoxyphenyl acetate, and 3,5-dimethoxyphenyl acetate; note Scheme XII. The observation was homolysis to give radical type products from the para isomer, a mixture of ionic and radical products from the meta isomer, and only ionic solvolysis photoproducts from the 3,5-dimethoxybenzyl acetate. Since the early computations were of the Hückel variety, it seemed proper to determine how different more modern



Scheme XI. The photochemical solvolytic behavior of the nitrophenyl trityl ethers. G = NO₂.



Scheme XII: The solvolytic behavior of the methoxybenzyl acetates.

computational technique would prove. Thus, Gaussian94 was employed to obtain the energies of the *p*-methoxybenzyl, the *m*-methoxybenzyl and 3,5-dimethoxybenzyl cations and radicals in their first excited states.⁴⁰ To this end, CASSCF(8,8)/6-31G*, as well as the CASSCF(10,10)/6-31G* for the 3,5-methoxy compound, were carried out with geometry optimization for both the benzylic cations and the radicals. Such computations are at the limit of present-day capabilities and required weeks for each such calculation. In order to consider the counterpart species, that is, the acetate counterion or the acetoxy counterpart radical, these were computed separately with these species being taken as ground state. The total energies are given in Table III.

It is seen from Table III that the preferences are in favor of the ion pairs and become more so as meta methoxy groups are introduced. The energy differences are small for the para isomer. However, it is important to recognize that the energies computed for the ion and radical pairs are useful in judging the energetic consequences of bond-stretching of the ion versus the homolytic type. This does not mean that the excited ion and radical pairs are actually obtained experimentally. This point is addressed when we consider the energy gaps between S_0 and S_1 for the different pairs. gaps are much larger, meaning that selectively for the meta ion pairs the excited surface has come closer to ground state.

Table III. CASSCF(8,8) energies of ion and radical pairs.

	Ion Pair	Radical Pair	Δ Rad vs Cation	Cation Δ	Radical Δ
Mono-meta	-610.14687	-610.11433	0.03254	0.01580	0.09161
Para	-610.12340	-610.11704	0.00635	0.05534	0.09438
Di-Methoxy	-724.05620	-724.00483	0.05137	0.00250	0.09395

Cation and radical pair energies are for S_1 . The energy units are hartrees (627.5 kcal/mole per hartree). Column 3 gives the energy favoring ionic versus homolytic dissociation. Columns 4 and 5 give the S_0 - S_1 energy gaps.

Further, this led to a rather exciting result. Gaussian94 contains methodology for computing conical intersections and avoided crossings. The case of the dimethoxybenzylic cation was studied using a CASSCF(8,8)/6-31G* conical computation which led to a geometry with a minimum energy separation of 0.15 kcal/mole. The separation for the mono methoxylated cation was slightly larger (circa 0.3 kcal/mole). These computations are of the "state averaging" type and lead to final energies for the S_0 - S_1 combination which are about 1/100th of a Hartree higher in energy than the optimized S_1 . This signifies that the geometry found for the conical intersection (or avoided crossing) is slightly different and displaced from the S_1 energy minimum.⁴¹

2.5 *The Large K - Small K Concept Controlling Multiplicity Dependent Reactions*

Often in organic photochemistry one encounters reactants which afford one product from the singlet excited state and a different one from the triplet. There is a generalization which we uncovered some years ago.⁴² The basic idea is that the singlet-triplet splitting in a photochemical transition state may vary widely. For a single configuration involving singly occupied HOMO and LUMO MO's, the splitting is given by twice the exchange integral, $G_{kl|lk}$ or K , between these two MO's [note Ref. 43, Chap. 5 for a discussion]. This splitting of $2K$ may be small or large. The two extremes are qualitatively depicted in Figure 12. Assuming that the center of gravity of the MO's does not differ appreciably, it can be seen that the T1 and S1 states will be positioned energetically similarly to that in Figure 12. It is also seen that if one can categorize two competing reactions as "small K" and "large K" reactions, then a triplet will find the lower energy hypersurface and path on the "large K" route. Conversely, a singlet will make use of the lower energy "small K" route. The problem is to categorize reactions in terms of the exchange integrals on the excited state hypersurfaces. For simplicity, if

one uses the zero differential overlap (i.e. ZDO) approximation, one can write the

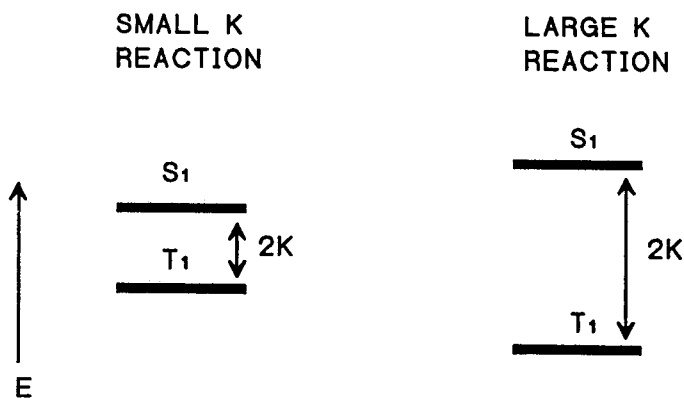


Figure 12: Large K - small K energetics.

exchange integral as the summation in Equation 5.

$$K = \sum_{r,s} [C_{rH} C_{rL} C_{sH} C_{sL} \gamma_{rs}] \quad (5)$$

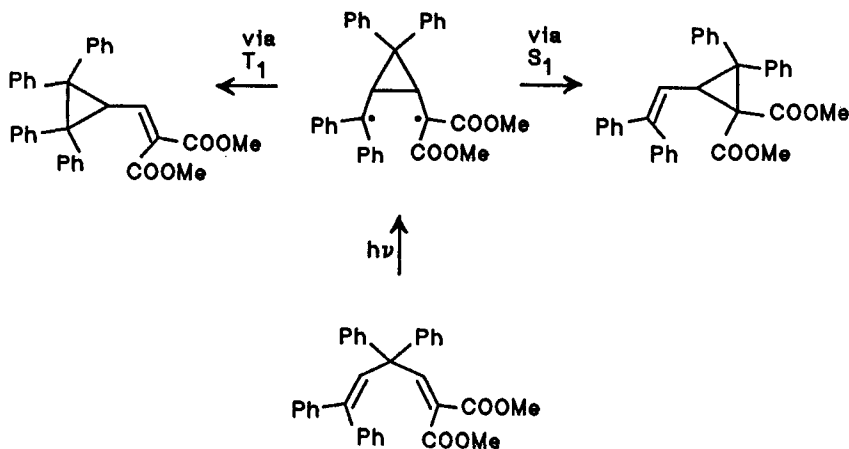
or in matrix notation:

$$K = \omega \Gamma \omega$$

Here the ω vector and its transpose ω have columns and rows, respectively, consisting of the terms $C_{iL} C_{iH}$. L and H refer to HOMO and LUMO MO's and r and s refer to basis hybrid or atomic orbitals. The Γ matrix has the elements γ_{rs} , that is, the repulsion integrals between basis orbitals r and s. Thus it is the magnitude of such triple products occurring in the summation of Equation 5 and these, in turn, depend on the proximity of basis orbitals r and s as well as the LCAO MO coefficients at centers r and s. Where HOMO and LUMO are heavily weighted at the same sites, and thus HOMO and LUMO "match" the exchange integral tends to be large. For highly polarized species, HOMO and LUMO tend not to have heavy weightings at the same centers, and a small K results. Also, for 4N and photochemically allowed pericyclic reactions, HOMO and LUMO for symmetry reasons, there is poor matching and a small K results. Diradical processes of non-polar species usually have the relevant MO's similar distributed and large K values

result.

A very simple example is that of butadienes which undergo an electro-cyclic ring closure to cyclobutenes from the singlet while the triplet excited state preferentially undergoes cis-trans isomerization about the π -bonds. A more complex case is the Di- π -Methane Rearrangement of the tetraphenyldiester shown in Scheme XIII. Here the usual cyclopropyldicarbonyl diradical is formed in the first step of the reaction. However, there are two alternative ways for this species to "unzip" and proceed onwards to photoproduct. The singlet, generated by "direct irradiation" (i.e. without addition of a sensitizer), leads to the product with carbomethoxy groups on the three-membered ring while the triplet, generated by use of a triplet sensitizer, affords the photoproduct with the ester groups on the double bond of product. The pathway leading onward to the singlet photoproduct retains the carbomethoxy groups at an odd-electron center as the three-ring opens. At this stage of the transformation, the diradicaloid species then is polarized and prefers a small K pathway from the singlet. However, in the case of the triplet, the alternative opening does not develop electron density on the electronegative ester group and prefers this large K pathway.



Scheme XIII: Differing singlet and triplet regioselectivities in a bicycle reaction.

2.6 *Delta-P and Delta-E Matrix Analysis*

An intriguing question is how an excited state differs from its ground state counterpart. Thus, how do the bond orders, the electron densities, and the geometry change? Additionally, how is the excitation energy distributed?

These questions have been addressed⁴⁴ with the definition of a ΔP matrix. This

matrix is defined as the difference between an excited state bond order or density matrix and the corresponding ground state one. Note Equation 6.

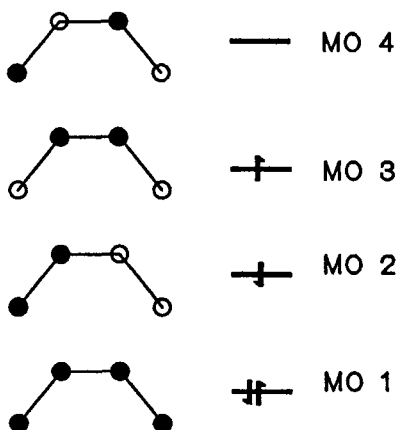
$$\Delta P = P^* - P_0 \quad (6)$$

The basic idea is that on excitation most of the bond orders tend to decrease, although some do increase. These changes are seen in the off-diagonal elements of the ΔP matrix. The diagonal elements give the changes in electron density resulting from excitation.

Thus, in a molecule such as n-octylnaphthalene one expects excitation to be heavily localized in the naphthyl chromophore and only slightly delocalized into the octyl side-chain. Thus, the ΔP matrix has appreciably sized elements corresponding to the atoms and bonds of the naphthyl group and only slightly in the octyl side chain. The method is applicable to any computations which affords Mulliken population analysis matrices or a density matrices.

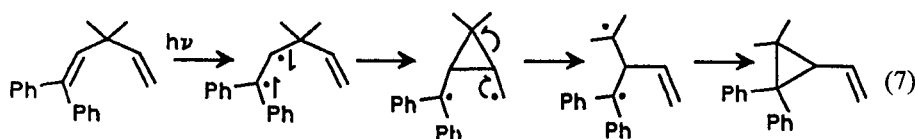
As noted, most off-diagonal elements of the ΔP matrix tend to be negative and these elements correspond to the distribution of excitation energy in making these bonds more antibonding. A simple case to consider in understanding the idea, is that HOMO-LUMO excitation of butadiene. This is depicted in Scheme XIV. It is seen that excitation involves promotion of an electron from an MO which is 1-2 and 3-4 bonding to one which is antibonding at these sites. However, the effect on bond 2-3 is the reverse. Thus, for such excited states of butadiene one can anticipate terminal double bond rotation and cis-trans isomerization if there are end substituents. Also one can expect rigidity and "freezing" of rotation about the middle π -bond.

With respect to energy distribution, we can see that the excitation energy is concentrated in π -bonds 1-2 and 3-4 while there is actually an energetic decrease in the energy of π -bond 2-3. Finally, we note that for simplicity the discussion has dealt only with the simple HOMO-LUMO excitation process and not with other excitation processes involving MO's 1 and 4. Finally, it is worth commenting that the method is particularly useful if one employs the Weinhold natural bond hybrids¹⁶ as a basis, since then excitation diffusing into any of the sigma bonds can be readily discerned.



Scheme XIV: HOMO-LUMO butadiene excitation bond order effects.

Beyond this, if one is computing the hypersurface for a reaction, the ΔP treatment may be applied at the various points of interest on the hypersurface. For example, the Di- π -Methane Rearrangement of the diphenyldimethyl-1,4 pentadiene in Equation 7 provides one interesting case.^{44c} As might be anticipated application of the ΔP matrix idea to the initial excited state, a singlet here, revealed that excitation is heavily localized in the diphenyl-vinyl moiety; this is the lowest energy chromophore in the molecule. However, as one moves along the reaction coordinate to the cyclopropyldicarbonyl species, the largest matrix elements correspond to bonds of the three-membered ring. In accord with this, inspection of the eigenvectors of the dicarbonyl diradical reveals typical benzhydryl radical type weightings, and it is the cyclopropyl dicarbonyl group which has been perturbed. Of course, it is unlikely that the molecule will proceed adiabatically to excited state of photoproduct, and along the hypersurface one expects decay to the S_0 surface. In any case, the migration of excitation during an excited state transformation is general.



2.7 *The Role of S₀-S₁-S₂ Mixing*

In discussions of excited states it is often considered that a simple HOMO-LUMO excitation process is involved. However, this is really not invariably the case, and in any event is an oversimplification. Configuration interaction leads to mixing of a variety of excited configurations in most situations. One simplification is to consider just three configurations. This is related to a point made by Oosterhof who commented that, although there is an avoided crossing of S₀ and S₂ in the photochemical cyclization of butadiene to cyclobutene and yet S₁ is the state of photochemical interest.⁴⁵ It has been shown by the present author^{44f,46} that there is S₀-S₁-S₂ mixing despite Brillouin's theorem which precludes S₀-S₁ interaction. We can assume some deviation from perfect symmetry (e.g. vibrationally). Thus, S₀ has a matrix interaction element with S₂, which is not precluded from mixing with S₁. The net result is that the three configurations interact in a fashion analogous to the interaction of the three linearly oriented p-orbitals of an allylic species (i.e. here S₀-S₂-S₁). However, in this case, unlike the interaction of the three atomic orbitals, the off-diagonal matrix elements are positive. Thus, the nodal character of the "linear" combination of the three configurations is inverted from that of the p-orbital case. The lowest energy resulting state has the weighting of S₀ - S₂ + S₁ and the highest energy state has all configurations weighted positively.

In the same work it was found that the Möbius-Hückel approximation still operates correctly in the ZDO-SCF approximation, thus justifying our earlier efforts based on Hückel theory (i.e. topology).

Conclusion

This survey has selected a limited number of situations where a theoretical analysis has been of value in the author's ground-state and photochemical research. A general conclusion is that both experimental exploration of chemical phenomena and theoretical interpretation of the observations, together, provide a satisfying mode of doing mechanistic research.

Acknowledgment

It is a pleasure to acknowledge the support of the National Science Foundation without which these studies would not have been possible.

References

1. A.J. Birch and D. Nasipuri, *Tetrahedron*, 148 (1959).
2. (a)A.P. Krapcho and A.A. Bothner-By, *J. Am. Chem. Soc.* **81**, 3658 (1959).
3. *Tetrahedron* **16**, 169 (1961).
4. (a)H.E. Zimmerman and P.A. Wang, *J. Am. Chem. Soc.* **112**, 1280 (1990).
(b)H.E. Zimmerman and P.A. Wang, *J. Am. Chem. Soc.* **115**, 2205 (1993).
5. (a)Gaussian 92, Revision A. M.J. Frisch, G.W. Trucks, M. Head-Gordon, P.M.W. Gill, M.W. Wong, J.B. Foresman, B.G. Johnson, H.B. Schlegel, M.A. Robb, E.S. Replogle, R. Gomperts, J.L. Andres, K. Raghvachari, J.S. Binkley, C. Gonzalez, R.L. Martin, D.J. Fox, D.J. Defrees, J. Baker, J.J.P. Stewart, J.A. Pople, Gaussian, Inc., Pittsburgh PA, 1992.
(b)Gaussian 90, Revision J, M.J. Frisch, M. Head-Gordon, G.W. Trucks, J.B. Foresman, H.B. Schlegel, K. Raghavachari, M. Robb, J.S. Binkley, C. Gonzalez, D.J. Defrees, D.J. Fox, R.A. Whiteside, R. Seeger, C.F. Melius, J. Baker, R.L. Martin, L.R. Kahn, J.J.P. Stewart, S. Topial, J.A. Pople, Gaussian Inc., Pittsburgh, PA, 1990.
(c)QPCE Program No. QG01, Quantum Chemistry Program Exchange, Indiana University; M.W. Schmidt, K.K. Baldrige, J.A. Boatz, J.H. Jensen, S. Koseki, M.S. Gordon, K.A. Nguyen, T.L. Windus, S.T. Elbert, QPCE Bull., August 1990, p. 10.
(d)Gaussian94, Revision. D.
6. H.E. Zimmerman in *Molecular Rearrangements*, ed. P. DeMayo (Interscience, New York, 1963), pp. 347-349; *ibid*, *idem*, pp. 346-347.
7. H.E. Zimmerman and A. Zweig, *J. Amer. Chem. Soc.* **83**, 1196 (1961).
8. H.E. Zimmerman, *Quantum Mechanics for Organic Chemists* (Academic Press, New York, 1975).
9. R.B. Woodward and R. Hoffmann, *J. Am. Chem. Soc.*, 395 (1965).
10. H.C. Longuet-Higgins and E.W. Abrahamson, *J. Am. Chem. Soc.*, 2045 (1965).
11. E. Heilbronner, *Tetrahedron Lett.*, 1923 (1964).
12. H.E. Zimmerman, *J. Amer. Chem. Soc.* **88**, 1564 (1966).
13. A.A. Frost and B. Musulin, *J. Chem. Phys.* **21**, 572 (1953).
14. For a discussion and original references see, A. Streitwieser, *Molecular Orbital Theory For Organic Chemists* (Wiley, New York, 1961).
15. H.E. Zimmerman and F. Weinhold, *J. Am. Chem. Soc.* **116**, 1579 (1994).
16. (a)J.P. Foster and F. Weinhold, *J. Am. Chem. Soc.* **102**, 7211 (1980).
(b)A. Reed, L.A. Curtiss and F Weinhold, *Chem. Rev.* **88**, 899 (1988).
17. (a)S. Winstein, H.M. Walborsky and K. Schreiber, *J. Am. Chem. Soc.* **72**, 5795 (1950).

- (b)S. Winstein and D.S. Trifan, *J. Am. Chem. Soc.* **74**, 1154 (1952).
18. (a)G.W. Wheland and D.W. Mann, *J. Chem. Phys.* **17**, 264 (1949).
(b)G. Wheland, *J. Am. Chem. Soc.* **64**, 900 (1942).
19. H.E. Zimmerman, unpublished.
20. MOPAC Vers. 6.1, QCPE #455.
21. (a)H.E. Zimmerman, Seventeenth National Organic Symposium of the Amer. Chem. Soc., Bloomington, Indiana, (1961), pgs. 31-41.
(b)H.E. Zimmerman and D.I. Schuster, *J. Amer. Chem. Soc.* **83**, 4486 (1961).
(c)H.E. Zimmerman and D.I. Schuster, *J. Amer. Chem. Soc.* **84**, 4527 (1962)
(d)H.E. Zimmerman, in *Advances in Photochemistry*, Eds. A. Noyes, Jr., G. S. Hammond and J. N. Pitts, Jr. (Interscience, Vol. 1, 1963), pp. 183-208.
22. M. Kasha, 1960 Radiation Res., Suppl. 2, 243; M. Kasha, in *Light and Life*, Eds. W.D. McElroy and B. Glass (Johns Hopkins Press, Baltimore, 1961).
23. (a)H.E. Zimmerman, D. Döpp and P.S. Huyffer, *J. Amer. Chem. Soc.* **88**, 5352 (1966).
(b)H.E. Zimmerman, D.S. Crumrine, D. Döpp and P.S. Huyffer, *J. Amer. Chem. Soc.* **91**, 434 (1969).
24. H.E. Zimmerman, R.W. Binkley, J.J. McCullough and G.A. Zimmerman, *J. Amer. Chem. Soc.* **89**, 6589 (1967).
25. H.E. Zimmerman and G.L. Grunewald, *J. Amer. Chem. Soc.* **88**, 183 (1966).
26. (a)H.E. Zimmerman, R.W. Binkley, R.W. Givens and M.A. Sherwin, *J. Amer. Chem. Soc.* **89**, 3932 (1967).
(b)H.E. Zimmerman, R.W. Binkley, R.S. Givens, M.A. Sherwin and G.L. Grunewald, *J. Amer. Chem. Soc.* **91**, 3316 (1969).
(c)H.E. Zimmerman, H.M. Sulzbach and M.B. Tollefson, *J. Am. Chem. Soc.* **115**, 6548 (1993).
27. R. Hoffmann and W.N. Lipscomb, *J. Chem. Phys.* **36**, 3489 (1962).
28. H.E. Zimmerman, D. Armesto, M.G. Amezua, T.P. Gannett and R.P. Johnson, *J. Am. Chem. Soc.* **101**, 6367 (1979).
29. H.E. Zimmerman, *J. Amer. Chem. Soc.* **88**, 1566 (1966).
30. H.E. Zimmerman, *Accounts of Chem. Res.* **5**, 393 (1972).
31. (a)H.A. Jahn and E. Teller, *Proc. Roy. Soc. Ser. A* **161**, 220 (1937).
(b)G. Herzberg and Longuet-Higgins, *Discuss. Faraday Soc.* **35**, 77 (1963).
(c)E. Teller, *J. Phys. Chem.* **41**, 109 (1937).
32. J. Michl, *Mol. Photochem.* 1972, 243-255, 257-286, 287-314.
33. H.E. Zimmerman and R.E. Factor, *J. Amer. Chem. Soc.* **102**, 3538 (1980).
34. (a)H.E. Zimmerman, *Topics in Current Chemistry* **100**, 45 (1982) Springer-Verlag, Heidelberg-New York.
(b)H.E. Zimmerman and R.E. Factor, *Tetrahedron* **37**, 125 (1981), Supplement 1.

- (c)H.E. Zimmerman and T. P. Cutler, *J. Org. Chem.* **43**, 3283 (1978).
35. See Reference 5. Revision D of Gaussian94 contains the conical code.
36. (a)M.A. Robb, F. Bernardi and M. Olivucci, *Pure App. Chem.* **67**, 783 (1995).
(b)M. Olivucci, In. Ragazos, F. Bernardi and M.A. Robb, *J. Am. Chem. Soc.* **115**, 3710 (1993).
37. E. Havinga, R.O. De Jong and W. Dorst, *Rec. Trav. Chim.* **75**, 378 (1956).
38. H.E. Zimmerman and S. Somasekhara, *J. Amer. Chem. Soc.* **85**, 922 (1963).
39. H.E. Zimmerman and V.R. Sandel, *J. Amer. Chem. Soc.* **85**, 915 (1963).
40. H.E. Zimmerman, *J. Am. Chem. Soc.* **117**, 8988 (1995).
41. H.E. Zimmerman, unpublished results.
42. (a)H.E. Zimmerman, J.H. Penn and M.R. Johnson, *Proc. Natl. Acad. Sci. USA*, **78**, 2021 (1981).
(b)H.E. Zimmerman, D. Armesto, M.G. Amezua, T.P. Gannett and R.P. Johnson, *J. Amer. Chem. Soc.* **101**, 6367 (1979).
(c)H.E. Zimmerman and R.E. Factor, Ref. 34b.
(d)H.E. Zimmerman, J.H. Penn and M.R. Johnson, *Proc. Natl. Acad. Sci. USA*, **78**, 2021 (1981).
(e)H.E. Zimmerman and G.-S. Wu, *Canadian J. Chem.* **61**, 866 (1983).
43. H.E. Zimmerman, *Quantum Mechanics for Organic Chemists* (Academic Press, New York, 1975).
44. (a)H.E. Zimmerman, W.T. Gruenbaum, R.T. Klun, M.G. Steinmetz and T.R. Welter, *J.C.S. Chemical Communications* (1978) 228-230.
(b)H.E. Zimmerman and T.R. Welter, *J. Amer. Chem. Soc.* **100**, 4131 (1978).
(c)H.E. Zimmerman and R.T. Klun, *Tetrahedron* **43**, 1775 (1978).
(d)H.E. Zimmerman and M.G. Steinmetz, *J.C.S. Chemical Communications*, (1978), 231-232.
(e)See References 33c and 42c.
(f)H.E. Zimmerman, *Accts. of Chem. Research*, **10**, 312 (1982).
(g)H.E. Zimmerman, J.H. Penn and C.W. Carpenter, *Proc. Natl. Acad. Sci. USA*, **79**, 2128 (1982).
45. W.Th.A.M. van der Lugt and L Oosterhoff, *J. Am. Chem. Soc.* **91**, 6042 (1969).
46. H.E. Zimmerman, *Tetrahedron* **38**, 753 (1982).